Power spectrum from weak-shear data

Matthias Bartelmann and Peter Schneider

Max-Planck-Institut für Astrophysik, P.O. Box 1523, D-85740 Garching, Germany (msb, peter@mpa-garching.mpg.de)

Abstract. We demonstrate that the aperture mass as a measure for cosmic shear closely approximates (to better than $\approx 5\%$) the scaled and shifted power spectrum of the projected mass density. This cosmological weak-lensing information can thus be used to directly infer the projected matter power spectrum with high accuracy. As an application, we show that aperture-mass observations can be used to constrain the cosmic density parameter and the power-spectrum amplitude. We show that, for a particular example, it should be possible to constrain Ω_0 to within $\approx \pm 27\%$, and σ_8 to within $\approx \pm 8\%$ using weak-shear data on a square-shaped field of $8°$ side length.

Key words: cosmology: observations – cosmology: dark matter – cosmology: gravitational lensing – cosmology: large-scale structure of Universe

1. Introduction

A new measure for cosmic shear, the aperture mass $\langle M_{\mathrm{ap}} \rangle$, was recently proposed by Schneider et al. (1998; hereafter S98). It was shown there that $\langle M_{\mathrm{ap}}^2 \rangle$ is related to the power spectrum P_κ of the projected density fluctuations filtered with a narrow function. Here, we demonstrate in Sect. 2 that an accurate approximation to $\langle M_{\mathrm{ap}}^2 \rangle$ can be constructed which directly yields P_κ. In essence, this makes the projected matter power spectrum a directly observable quantity, so that no deconvolution algorithms need to be invoked. We then use our approximation in Sect. 3 to infer the cosmic density parameter Ω_0 and the power-spectrum normalisation σ_8 from simulated data. We present our conclusions in Sect. 4.

2. Aperture mass and approximations

2.1. Effective convergence

The two-point statistics of the gravitational lens properties of the large-scale structure can be described, to high accuracy, in terms of the power spectrum of an equivalent single lens plane matter distribution (see, e.g., Kaiser 1998; S98; and references therein), which is given by

$$P_\kappa(l) = \frac{9 H_0^4 \Omega_0^2}{4 c^4} \int_0^{w_{\mathrm{H}}} \mathrm{d}w \frac{W^2(w)}{a^2(w)} P_\delta\left(\frac{l}{f_K(w)}, w\right) , \quad (1)$$

where l is the Fourier conjugate to the angle $\boldsymbol{\theta}$, w and $f_K(w)$ are the comoving radial and angular-diameter distance, respectively, $a = (1+z)^{-1}$ is the scale factor, $P_\delta(k, w)$ is the density-perturbation power spectrum, and $W(w)$ is the weight function

$$W(w) = \int_w^{w_{\mathrm{H}}} \mathrm{d}w' G(w') \frac{f_K(w' - w)}{f_K(w')} , \quad (2)$$

which depends on the probability distribution $G(w)$ of source distances. The upper integration limit w_{H} is the comoving horizon distance, here defined as the comoving distance corresponding to redshift infinity. Quite intuitively, Eq. (1) relates the lensing power on angular scales $\theta = 2\pi l^{-1}$ to the power in density fluctuations at a comoving scale $2\pi k^{-1} = f_K(w)\theta$.

We parameterise the source-distance distribution $G(w)$ as a function of redshift, $G_z(z)$, specified by

$$G_z(z) = \frac{\beta}{z_0^3 \Gamma(3/\beta)} z^2 \exp\left[-\left(\frac{z}{z_0} \right)^\beta \right] . \quad (3)$$

It is normalised to $0 \leq z < \infty$ and provides a good fit to the observed redshift distribution (e.g. Smail et al. 1995). The mean redshift $\langle z \rangle$ is proportional to z_0. For $\beta = 1.5$ which we assume throughout, $\langle z \rangle \approx 1.505 \, z_0$.

2.2. Aperture mass

The aperture mass $M_{\mathrm{ap}}(\theta)$ as a function of smoothing scale θ is defined in terms of a weighted average within a circle of radius θ of the surface mass density of the equivalent single lens plane. It can readily be obtained from the observed image ellipticities of faint background galaxies which provide an unbiased estimate of the shear γ,

$$M_{\mathrm{ap}}(\theta) = \int \mathrm{d}^2 \vartheta \, Q(|\boldsymbol{\vartheta}|) \, \gamma_{\mathrm{t}}(\boldsymbol{\vartheta}) , \quad (4)$$

by replacing the integral over the shear by a sum over galaxy ellipticities. Here, γ_{t} is the tangential component of the shear relative to the aperture centre, and Q is an appropriately chosen weight function which is non-zero only for $0 \leq \vartheta \leq \theta$. The mean-squared aperture mass is related to the effective-convergence power spectrum through

$$\langle M_{\mathrm{ap}}^2 \rangle(\theta) = 2\pi \int_0^\infty \mathrm{d}l \, l \, P_\kappa(l) \, J^2(l\theta) , \quad (5)$$

where $J(\eta)$ is related to the filter function Q (see S98). For

$$Q(\vartheta) = \frac{6}{\pi} \frac{\vartheta^2(\theta^2 - \vartheta^2)}{\theta^6} \quad \Rightarrow \quad J(\eta) = \frac{12}{\pi\eta^2} \, \mathrm{J}_4(\eta) \; , \tag{6}$$

and $\mathrm{J}_4(\eta)$ is the fourth-order Bessel function of the first kind. $J^2(\eta)$ peaks at $\eta_0' \approx 4.11$. Examples for the *rms* aperture mass $\langle M_{\mathrm{ap}}^2 \rangle^{1/2}$ are plotted in Fig. 2 as a function of aperture radius θ.

It is crucial in Eqs. (1) and (5) to take the non-linear evolution of the density power spectrum into account. For aperture radii of order a few arc minutes, $\theta \approx 3 \times 10^{-4} \, \mathrm{rad}$, the peak η_0' of $J^2(\eta)$ translates to $l \approx 1.4 \times 10^4$, which corresponds to $2\pi k^{-1} \approx 1 \, h^{-1}\mathrm{Mpc}$ for sources around redshift unity, i.e. the physical scales of density perturbations to which the aperture mass is most sensitive to are well in the non-linear regime of evolution. We assume a CDM power spectrum and describe its non-linear evolution as given by Peacock & Dodds (1996). We normalise the spectrum to the local abundance of rich clusters by choosing σ_8 as derived by Viana & Liddle (1996) and Eke et al. (1996).

2.3. Signal-to-noise ratio

Although an *rms* aperture-mass amplitude around one per cent appears low, the signal-to-noise ratio of the aperture mass can be quite high. There are three sources of noise in a measurement of $\langle M_{\mathrm{ap}}^2 \rangle$. Since it will be inferred from distortions of galaxy ellipticities, the intrinsic non-vanishing ellipticity of the galaxies provides one source of noise, and the random positions of the galaxies provides another. The third source of noise is due to cosmic variance. Assuming a large number of galaxies N per aperture, and neglecting the kurtosis of the aperture mass, the dispersion of M_{ap} in a *single* aperture is (see S98)

$$\sigma^2(M_{\mathrm{ap}}^2) \approx \left(\frac{6\sigma_\epsilon^2}{5\sqrt{2}N} + \sqrt{2}\langle M_{\mathrm{ap}}^2 \rangle \right)^2 \; , \tag{7}$$

where $\sigma_\epsilon \approx 0.2$ is the intrinsic dispersion of the galaxy ellipticities. On angular scales of a few arc minutes and smaller, the galaxies dominate the noise, while the cosmic variance dominates on larger scales. Of course, M_{ap} will be measured in a large number of apertures N_{ap} rather than a single one. If the apertures are independent, the dispersion (7) is reduced by a factor of $N_{\mathrm{ap}}^{1/2}$, and the ensemble variance becomes

$$\bar{\sigma} = \frac{\sigma(M_{\mathrm{ap}}^2)}{N_{\mathrm{ap}}^{1/2}} \; . \tag{8}$$

Typical signal-to-noise ratios reach values of $\gtrsim 5$ for aperture radii of a few arc minutes and data fields of a square degree in size.

2.4. Approximate rms aperture mass

The strong peak of $J^2(\eta)$ – see Fig. 2 in S98 – motivates the approximation of J^2 by a delta function,

$$J^2(\eta) \approx A \, \delta_{\mathrm{D}}(\eta - \eta_0) \; , \tag{9}$$

with $A = 512/(1155\pi^3) \approx 1.43 \times 10^{-2}$, $\eta_0 = 693\pi/512 \approx 4.25$, as determined from the norm and mean of J^2.[1] Then the expression for the aperture mass (5) becomes particularly simple,

$$\langle M_{\mathrm{ap}}^2 \rangle(\theta) \approx \langle \tilde{M}_{\mathrm{ap}}^2 \rangle(\theta) \equiv 6(5\pi)^{-1} \, \theta^{-2} \, P_\kappa(\eta_0/\theta) \; . \tag{10}$$

If this provides a good approximation, the observable *rms* aperture mass at angular scale θ would directly yield the effective-convergence power spectrum $P_\kappa(l)$ at wave number η_0/θ, and thus a most direct and straightforward measure for dark-matter fluctuations. We therefore have to investigate whether replacing the filter function $J^2(\eta)$ by a delta function can be justified.

Let us first assume that $P_\kappa(l)$ can be approximated locally as a power law in l over a range in which J^2 differs significantly from zero,

$$P_\kappa(l) = B \, l^{n_{\mathrm{eff}}} \; . \tag{11}$$

Then, the true aperture mass (5) becomes

$$\langle M_{\mathrm{ap}}^2 \rangle(\theta) = \frac{144B}{\pi^{3/2}} \frac{\Gamma\left(\frac{3-n_{\mathrm{eff}}}{2}\right) \Gamma\left(3 + \frac{n_{\mathrm{eff}}}{2}\right)}{\Gamma\left(2 - \frac{n_{\mathrm{eff}}}{2}\right) \Gamma\left(6 - \frac{n_{\mathrm{eff}}}{2}\right)} \theta^{-(2+n_{\mathrm{eff}})} \; , \tag{12}$$

where the Gamma functions arise from integrating the power-law spectrum times the squared fourth-order Bessel function. The approximate aperture mass $\langle \tilde{M}_{\mathrm{ap}}^2 \rangle$ defined in Eq. (10) becomes

$$\langle \tilde{M}_{\mathrm{ap}}^2 \rangle(\theta) = 6(5\pi)^{-1} B \, \eta_0^{n_{\mathrm{eff}}} \, \theta^{-(2+n_{\mathrm{eff}})} \; . \tag{13}$$

The relative deviation of the approximation from the true aperture mass is a function of the effective power-law exponent n_{eff} only. It is plotted in Fig. 1. Clearly, the deviation of $\langle M_{\mathrm{ap}}^2 \rangle$ from $\langle \tilde{M}_{\mathrm{ap}}^2 \rangle$ is very small, less than five per cent, for effective power-spectrum slopes in the range $-1.5 \lesssim n_{\mathrm{eff}} \lesssim 0.5$, and this is exactly the range of slopes in the l interval contributing most of the power to the aperture mass for aperture radii of $\gtrsim 1'$. It is therefore fair to say that, especially in the presence of measurement errors, the aperture mass and its approximation (10) can be considered equivalent. Fig. 2 shows $\langle M_{\mathrm{ap}}^2 \rangle$ and $\langle \tilde{M}_{\mathrm{ap}}^2 \rangle$ for three cluster-normalised CDM models as examples for realistic non-power-law spectra, and emphasises the conclusions from Fig. 1. The approximation (10) to the aperture mass is excellent. This immediately implies that measurements of the aperture mass directly measure the effective-convergence power spectrum, and therefore the latter effectively becomes an observable quantity,

$$P_\kappa(l) \approx (5\pi/6) \, (\eta_0/l)^2 \, \langle M_{\mathrm{ap}}^2 \rangle(\eta_0/l) \; . \tag{14}$$

This provides the most straightforward access to a quantity of paramount importance for cosmology, i.e. the dark-matter power spectrum.

---

[1] In fact, the peak of $J^2(\eta)$ can well be approximated by a Gaussian. A least-square fit of a Gaussian to $J^2(\eta)$ yields

$$J^2(\eta) \approx A' \exp\left[-(\eta - \eta_0')^2/(2\sigma^2)\right]$$

with mean $\eta_0' \approx 4.11$, amplitude $A' \approx 4.52 \times 10^{-3}$, and variance $\sigma \approx 1.24$. The small width of the Gaussian encourages the approximation (9).
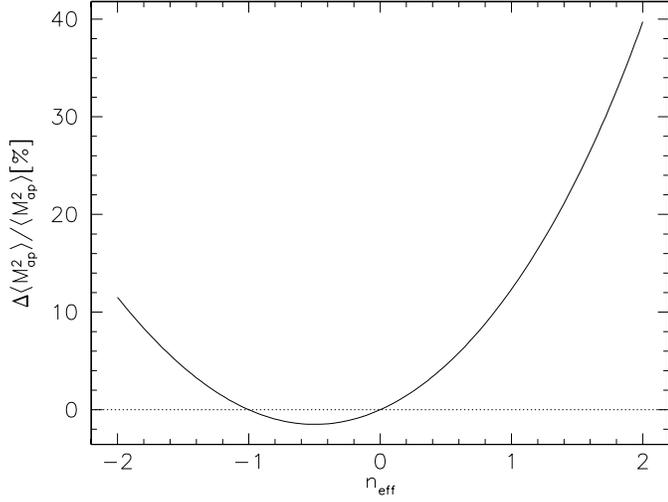
Fig. 1. Relative deviation between the true aperture mass $\langle M_{\rm ap}^2 \rangle$ and the approximate aperture mass $\langle \tilde{M}_{\rm ap}^2 \rangle$ as defined in Eq. (10), for an assumed effective-convergence power spectrum that is a power law in l. For the most relevant range of effective power-law exponents, $-1.5 \lesssim n_{\rm eff} \lesssim 0.5$, the relative deviation is less than five per cent.

3. Applications

It is now interesting to investigate a specific application of our results. Let us assume we are given a large, quadratic data field of angular size L, into which we place apertures of radius θ. We can place apertures of a fixed size densely on the field since the correlation of the aperture mass in neighbouring apertures is very small due to the narrowness of the filter function $J^2(\eta)$ (see Fig. 8 in S98). However, we want to sample $\langle M_{\rm ap}^2 \rangle$ at a variety of aperture sizes rather than a single one. Starting from a smallest aperture radius θ_0, we choose the next largest aperture radius as $\sqrt{2}\theta_0$ and so forth, so that consecutive aperture radii encompass on average twice as many galaxies. Clearly, the data for different aperture sizes are not completely uncorrelated, but decorrelate quickly with differing radius and centre separation – see again Fig. 8 of S98. Therefore, we assume that the number of independent apertures of radius θ is given by $N_{\rm ap} = [L/(2\theta)]^2$, and the expected number of galaxies per aperture is $N = n\pi\theta^2$. We assume a galaxy density of $n = 30$ per square arc minute. The expectation value of $\langle M_{\rm ap}^2 \rangle(\theta)$ is given by Eq. (5). Its 1-σ error at fixed aperture radius is expected to be given by Eq. (8). We show examples of simulated measurements M_i together with their expected 1-σ error bars in Fig. 3 for field sizes of $4°$ and $8°$.

Let M_i be the measurement of $\langle M_{\rm ap}^2 \rangle$ for aperture radius θ_i, then (8) yields the expected error of M_i. We can then try and fit the ensemble of measurements with the approximate aperture mass $\langle \tilde{M}_{\rm ap}^2 \rangle$. For that purpose, we define the χ^2 function

$$\chi^2 = \frac{1}{N_\theta} \sum_{i=1}^{N_\theta} \frac{[M_i - \langle \tilde{M}_{\rm ap}^2 \rangle(\theta_i)]^2}{\bar{\sigma}_i^2} \ . \tag{15}$$

As an example, we assume that data points like those shown in Fig. 3 have been measured in a cluster-normalised, low-density
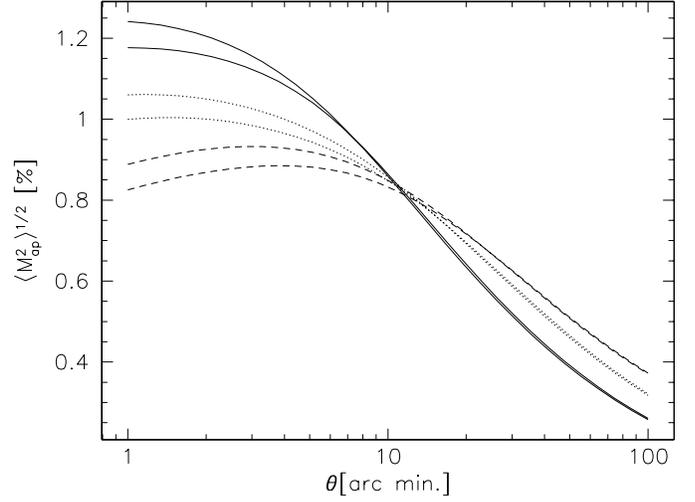

Fig. 2. Exact and approximate *rms* aperture masses $\langle M_{\rm ap}^2 \rangle$ and $\langle \tilde{M}_{\rm ap}^2 \rangle$ are shown for three cosmological models. All are cluster-normalised CDM models in which the non-linear growth of the density power spectrum P_δ was taken into account. Solid curves: low-density, open model ($\Omega_0 = 0.3$, $\Omega_\Lambda = 0$, $h = 0.7$); dotted curves: low-density, spatially flat model ($\Omega_0 = 0.3$, $\Omega_\Lambda = 0.7$, $h = 0.7$); dashed curves: Einstein-de Sitter model ($\Omega_0 = 1$, $\Omega_\Lambda = 0$, $h = 0.5$). The redshift distribution (3) of the sources was used. Typical *rms* aperture masses reach ~ 1 per cent at angular scales of a few arc minutes. The normalisation to the local abundance of rich clusters causes the curves to be very similar for the different choices of the cosmological parameters. While the approximate aperture mass slightly underestimates the true aperture mass at small aperture radii, $\theta \gtrsim 1'$, by at most $\approx 5\%$, the approximations fall exactly on top of the true curves for angular scales beyond $\approx 10'$.
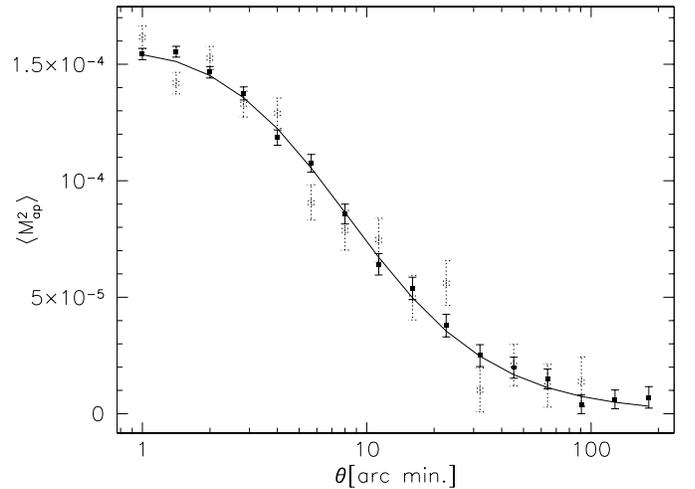

Fig. 3. Simulated aperture-mass measurements employing the sampling strategy detailed in the text. The error bars show 1-σ errors derived from Eq. (8). Field sizes of $4°$ and $8°$ were assumed for the open squares with dotted error bars and the filled squares with solid error bars, respectively. The true aperture mass is shown as the solid curve. The low-density, open CDM model was assumed for this plot, and $z_0 = 1$ was chosen for the redshift distribution of the sources. According to Eq. (10), the effective-convergence power spectrum can directly be read off from this plot.
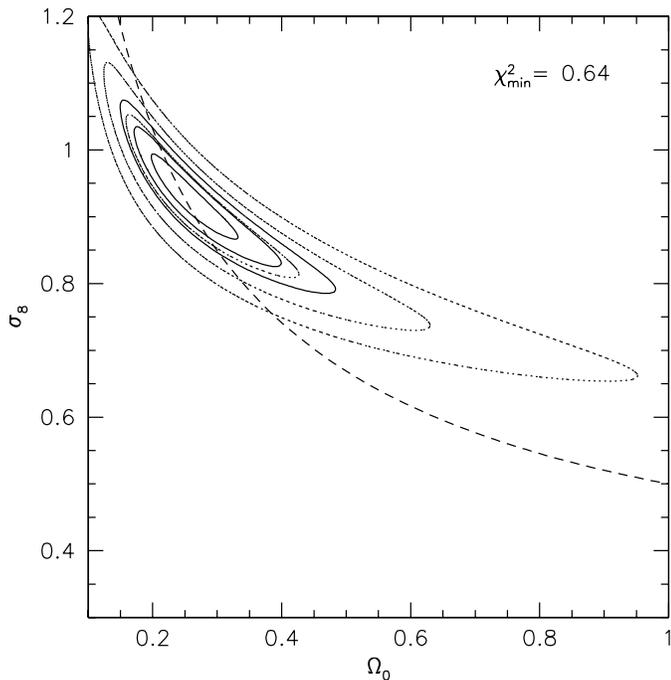
Fig. 4. Contours of χ^2 as defined in Eq. (15) are shown in the $\Omega_0 - \sigma_8$ plane. Input data and their errors were simulated as detailed in the text, assuming quadratic data fields of side length $4°$ and $8°$ (dotted and solid contours, respectively). Contours are shown for 1, 2, and 3-σ significance levels. The input cosmological model was the cluster-normalised, low-density, open CDM model with $\Omega_0 = 0.3$, $\Omega_\Lambda = 0$ and $h = 0.7$. Due to the cluster normalisation, $\sigma_8 = 0.85$. $\Omega_\Lambda = 0$ was assumed for the fit. The contours show that data on a $8° \times 8°$ field are sufficient to constrain Ω_0 at the 1-σ level to within $0.18 \lesssim \Omega_0 \lesssim 0.34$, and the amplitude to $0.85 \lesssim \sigma_8 \lesssim 0.99$. The long-dashed curve shows the present-day cluster-abundance constraint on Ω_0 and σ_8.

open CDM model. Assuming the CDM shape of the density-perturbation power spectrum, we can then vary parameters such as to minimise (15). The sensitivity of the aperture mass to the Hubble constant is very small. The remaining parameters are then the parameters β and z_0 of the source redshift distribution, the amplitude of the power spectrum, parameterised by σ_8, the density parameter Ω_0, and the cosmological constant Ω_Λ. It can safely be assumed that the redshift distribution $G(w)$ of background galaxies is known with high accuracy from other observations. We can therefore restrict ourselves to essentially two free parameters, σ_8 and Ω_0, and choose either $\Omega_\Lambda = 0$ or $\Omega_\Lambda = 1 - \Omega_0$. χ^2 contours for the former case are shown in Fig. 4.

The solid contours in the left panel of Fig. 4 show that at the 1-σ significance level, Ω_0 and σ_8 can be constrained to relative accuracies of $\approx \pm 27\%$ and $\approx \pm 8\%$, respectively. Table 1 gives 1-σ limits for fields of $4°$ and $8°$ side length. Similar experiments using $\Omega_\Lambda = 1 - \Omega_0$ instead of $\Omega_\Lambda = 0$ yield a minimum $\chi^2 \gtrsim 10$, so that spatially flat cosmologies can be rejected at very high significance using the data simulated with $\Omega_\Lambda = 0$.

Of course, the quality of the results depends on how accurately we guess the shape of the true power spectrum. For the

Table 1. 1-σ limits to Ω_0 and σ_8 obtained with fields of $4°$ and $8°$ side length.

	Ω_0		σ_8	
L	input	fit	input	fit
$4°$	0.3	0.25 ± 0.12	0.85	0.93 ± 0.12
$8°$	0.3	0.26 ± 0.08	0.85	0.93 ± 0.08

contours in Fig. 4, we vary two parameters and keep all others fixed. In Fig. 4 for example, we keep $h = 0.7$ constant, so that the shape parameter $\Gamma \equiv \Omega_0 h$ of the power spectrum is $\Gamma = 0.7\Omega_0$. If we would set the shape parameter instead to $\Gamma' = f\Gamma$ with $f \neq 1$, the best-fitting parameter combination (Ω_0, σ_8) would shift towards $f\Omega_0$ along the "valley" indicated by the χ^2 contours without substantially degrading the quality of the fit. This degeneracy reflects the degeneracy in the cluster abundance used to normalise the power spectrum for simulating the input data, because $\langle M_{\mathrm{ap}}^2 \rangle^{1/2}$ essentially measures the halo abundance at intermediate redshifts, $z \sim 0.3$. To illustrate this point, we indicate the present-day cluster-abundance constraint as the long-dashed curve in Fig. 4. It is seen to follow well the "valley" in the χ^2 contours for low Ω_0, but it departs increasingly for increasing Ω_0 because structure grows more rapidly between $z \sim 0.3$ and today for higher Ω_0. The parameter degeneracy with the cosmological constant can be broken using the skewness of M_{ap}, for which the degeneracy between Ω_0 and Ω_Λ is different (Van Waerbeke et al. 1999).

Although our assumptions concerning the number of independent apertures that can be placed inside a given data field and the neglect of the kurtosis in the approximation for $\sigma(M_{\mathrm{ap}}^2)$ may be slightly optimistic, we believe that these effects do not change our conclusions appreciably. It should be noted that for applying our technique, the data field need not be a connected region, but arbitrarily placed smaller areas on the sky with about equal total solid angle are equally useful. The rapid evolution towards square-degree CCD cameras at the best observing sites leaves us highly optimistic concerning the future application of our method.

4. Conclusions

We have shown here that a recently proposed measure for cosmic shear, the dispersion of the aperture mass $\langle M_{\mathrm{ap}}^2(\theta) \rangle$, can be approximated by the local value of the power spectrum P_κ of the projected matter fluctuations at wave number η_0/θ to a relative accuracy better than 5%. This is possible because the aperture mass is a convolution of P_κ with a narrow filter function which for this purpose can safely be approximated by a Dirac delta function.

In contrast to other methods for constraining $P_\kappa(l)$ through cosmic-shear data (Kaiser 1998; Seljak 1998; Van Waerbeke et al. 1999), the aperture-mass method allows for a simple combined analysis of independent data fields scattered across the sky. Furthermore, since $\langle M_{\mathrm{ap}}^2 \rangle^{1/2}$ is a scalar quantity directly obtained from observed galaxy-image ellipticities, its full

probability-distribution function can be derived and used for parameter extraction.

The approximate aperture mass can then straightforwardly be applied to constrain cosmological parameters from observed aperture masses. We simulated observations of $\langle M_{\mathrm{ap}}^2 \rangle$ and their expected errors and showed that Ω_0 and σ_8 can be recovered with relative accuracies of $\approx \pm 27\%$ and $\approx \pm 8\%$, respectively, using weak-shear data on a square field with $8°$ side length. For that, we have assumed that the parameters of the source redshift distribution are sufficiently well known. We believe that this is not a serious limitation because of the high reliability and accuracy of photometric redshift determinations (e.g., Benítez 1998, and references therein). In fact, the source-redshift dependence of $\langle M_{\mathrm{ap}}^2 \rangle$ can be used as a consistency check: With increasing source redshift, $\langle M_{\mathrm{ap}}^2 \rangle$ *increases*, while the skewness of M_{ap} *decreases*.

References

Benítez N., 1998, preprint astro-ph/9811189
Eke V.R., Cole S., Frenk C.S., 1996, MNRAS 282, 263
Kaiser N., 1998, ApJ 498, 26
Peacock J.A., Dodds S.J., 1996, MNRAS 280, L19
Schneider P., van Waerbeke L., Jain B., Kruse G., 1998, MNRAS 296, 873 (S98)
Seljak U., 1998, ApJ 506, 64
Smail I., Hogg D.W., Yan L., Cohen J.G., 1995, ApJ 449, L105
Van Waerbeke L., Bernardeau F., Mellier Y., 1999, A&A 342, 15
Viana P.T.P., Liddle A.R., 1996, MNRAS 281, 323